# STRUCTURAL STABILITY IN POWER SYSTEMS - EFFECT OF LOAD MODELS

M. A. Pai and P. W. Sauer
University of Illinois
Dept. of ECE
Urbana, IL

B. C. Lesieutre
M.I.T.
Dept. of EE & CS
Cambridge, MA

R. Adapa
E.P.R.I.
Elect. Sys.
Palo Alto, CA

## Abstract

In this paper a new notion of power system stability, is introduced, namely structural stability, and its significance in the context of load modeling is examined. It is shown that beyond certain values of load indices in the case of static models and beyond certain value of the dynamic component in the load such as induction motors, the system may become structurally unstable. The immediate application of these results is in the voltage stability problems.

## 1 Introduction

In this paper we investigate structural stability in power systems. Broadly speaking structural stability refers to the domain in the parameter space such that for small variations in the parameter vector inside the domain, the phase portrait does not change qualitatively. In Lyapunov stability we analogously talk about the region of attraction of an equilibrium point in the state space such that for any initial condition in the region the trajectory approaches the equilibrium point asymptotically. While considerable research has been done in the Lyapunov stability area, comparatively very little has been done in the structural stability area. It was partly because of the inability to formulate theorems and condition for structural stability in $n$ dimensional space. However, research in bifurcation theory has thrown up an intimate connection between it and structural stability. Stability regions in the parameter space or under continuous structural variations with respect to time (topology, load demands, nature of load, etc) are of interest.

In this paper it is shown that when a system loses structural stability we have bifurcation either local or global. Steady-state stability and voltage stability are used as illustrations for the physical system.

It is expected that this attempt at quantitatively applying structural stability to power systems will complement the work of Lyapunov stability via energy functions that has successfully been applied in power systems over the last five decades.

This paper was presented at the 1993 Athens Power Tech Conference held in Athens, Greece, September 5–8, 1993.

## 2 Structural Stability

The notion of structural stability was first proposed by Andronov and Pontryagin in 1937 [1]. The basic idea is that under small perturbations, dynamical systems must preserve their topological behavior to be structurally stable. From a simulation point of view it is nice for a dynamical system to have this property. Dynamical systems can never be modeled exactly due to measurement errors, etc, and moreover the finite precision of computers and the errors of floating point arithmetic will introduce additional sources of uncertainty. Thus the system that is being simulated is a perturbed version of the exact system. If the system is structurally stable then these errors will affect the simulation only marginally.

Mathematically, structural stability has to do with examining the change in qualitative behavior of a nonlinear dynamical system

$$\dot{x} = f(x) \tag{1}$$

as we change the vector field $f$. If the qualitative behavior remains the same for all nearby vector fields then the system (1) is said to be ***structurally stable*** [2]. References [2-5] discuss structural stability in a rigorous mathematical framework. Refs. [6-7] discuss it in an engineering context.

### 2.1 Result For Planar Systems [2-5]

Let $f$ in (1) be a $C^1$ vector field on a compact, two-dimensional, differentiable manifold $M$. Then $f$ is ***structurally stable*** on $M$ if and only if

1. The number of equilibrium points and limit cycles of (1) is finite and each is hyperbolic. An equilibrium point is hyperbolic if the linearized system at the equilibrium point has no eigenvalues on the imaginary axis.
2. There are no trajectories connecting saddle points.
3. The set $M$ consists of equilibrium points and limit cycles only.

### 2.2 Numerical Example

The post-fault swing dynamics of a single machine infinite bus system is given by

$$.0138\frac{d^2\delta}{dt^2} + D\frac{d\delta}{dt} = 0.91 - 3.02\sin\delta + .416\sin 2\delta \tag{2}$$

If we vary $D$ only, the number of equilibrium points remain the same. Furthermore as we vary $D$ over a wide range of values even the nature of equilibrium points remain the same.

However the global phase portrait changes qualitatively at a critical value of $D$. This is shown in Figs. 1(a), (b) and (c), where at the critical value of $D = .04687$, there is a trajectory connecting two saddle points. From property 2 of Sec. 2.1, the system is not structurally stable at this point since the phase portrait for $D <$ or $> .04687$, is qualitatively different. Notice that for large $D$ (Fig. 1(c)), both the left and right unstable equilibrium points lie on the boundary of the region of attraction of the stable equilibrium point. For small $D$ (Fig. 1(b)), only the right unstable equilibrium point lies on the boundary of the region of attraction of the stable equilibrium point. The critical case (Fig. 1(a)) is the point where this change occurs. In contrast to local bifurcation, this is called global bifurcation [5]. An analytical expression for this can be obtained using Fourier series [8].

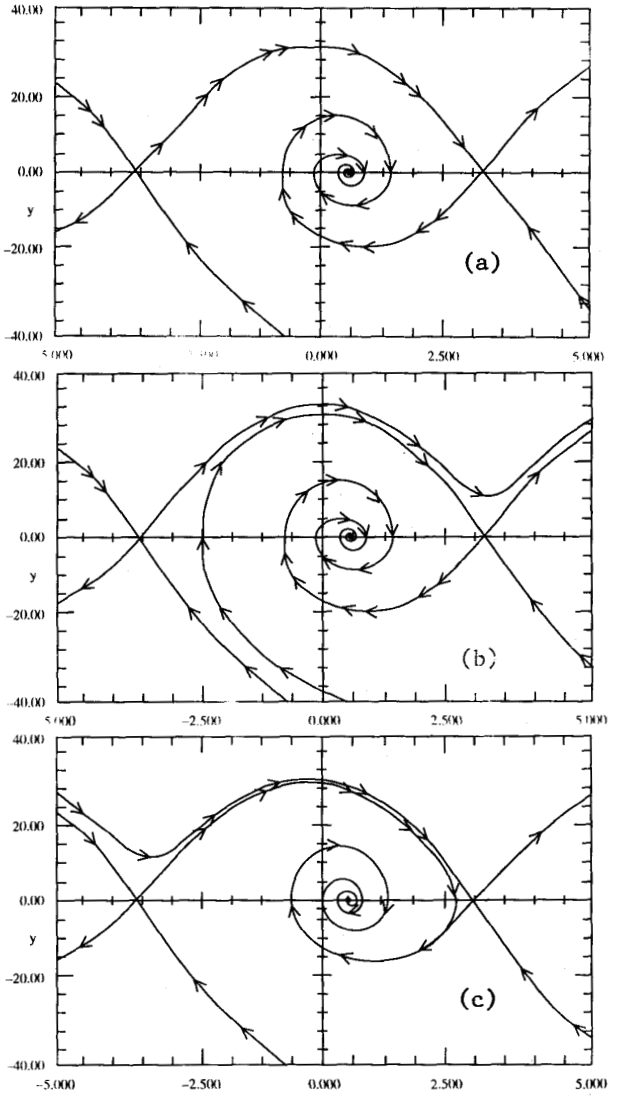


Figure 1: Phase portraits for different values of damping $D$: (a) $D = .04687$ (b) $D = .04$ (c) $D = .05$

# 3 Application In Multimachine Systems With Static Nonlinear Loads

In normal operation, a power system is structurally stable since the operator steers the system with a safe margin. Under stressed conditons this margin may get smaller. We wish to know the critical value of a parameter such as the load, which if increased incrementally will result in one or a pair of eigenvalues crossing over to the right half plane. This is the point of local bifurcation and the system is structurally unstable at this point. The analysis is done via small signal analysis of power systems [9-11], and it is the principal tool to study both low-frequency oscillations and voltage stability.

The system equations are of the form [12]

$$\dot{x} = f(x, y, u, p) \quad (3)$$

$$0 = g(x, y, p) \quad (4)$$

$y$ is the set of algebraic variables of the network power flow equations and generator currents $I_d$, $I_q$. $p$ is the parameter vector and $u$ the input vector. For stability analysis we form the linearized system. The overall linear dynamic model after eliminating the generator currents and incorporating voltage dependency of the load is obtained as

$$\begin{bmatrix} \Delta\dot{x} \\ 0 \\ 0 \end{bmatrix} = \begin{bmatrix} \tilde{A}_1 & \tilde{A}_2 & \tilde{A}_3 \\ \tilde{B}_1 & \tilde{B}_2 & \tilde{B}_3 \\ \tilde{C}_1 & \tilde{C}_2 & \tilde{C}_3 \end{bmatrix} \begin{bmatrix} \Delta x \\ \Delta z \\ \Delta v \end{bmatrix} + \begin{bmatrix} E \\ 0 \\ 0 \end{bmatrix} \Delta U \quad (5)$$

where $[\Delta z^T \mid \Delta v^T] = [\Delta\theta_1, \Delta V_1, ..., \Delta V_m \mid \Delta\theta_2, ..., \Delta\theta_n, \Delta V_{m+1}, ..., \Delta V_m]$. $\Delta v$ is the set of traditional load flow variables.

Now $\tilde{C}_3$ is the load flow Jacobian $J_{LF}$ and $\begin{bmatrix} \tilde{B}_2 & \tilde{B}_3 \\ \tilde{C}_2 & \tilde{C}_3 \end{bmatrix} = J_{AE}$ is defined as the algebraic Jacobian in [11]. The system A matrix is obtained as

$$\Delta\dot{x} = A_{sys}\Delta x + E\Delta U \quad (6)$$

where

$$A_{sys} = \tilde{A}_1 - [\tilde{A}_2 \quad \tilde{A}_3][J_{AE}]^{-1} \begin{bmatrix} \tilde{B}_1 \\ \tilde{C}_1 \end{bmatrix} \quad (7)$$

For the 3-machine case [13] the results are summarized in Table 1 for increasing constant power loading at bus 5. The last column indicates the states associated with the critical mode using participation factor analysis [14]. The model is a two axis model with an IEEE Type I exciter. The complete equations are available in Refs. [11-12] with the minor change of neglecting turbine governor dynamics. The equations are omitted for lack of space.

When the load is increased, it is observed that the critical modes for the unstable eigenvalues are the electrical ones associated with the excitation system ($E'_q$ and $R_f$). From Table 1 we observe that when the load at bus 5 is increased from 4.7 pu to 4.8 pu, the complex pair of unstable eigenvalues splits into real ones which move in the opposite directions along the real axis. The one moving along the positive real axis (9.2464) is sensitive to the rotor angle mode and eventually comes back to the left-half plane via $+\infty$ when the load at bus 5 is increased from 4.8 pu to 4.9 pu. This is the point when $\det J_{AE}$ changes sign. This is the point of singularity induced bifurcation. The other unstable real eigenvalue moves to the left

Table 1: Modal Behaviour for Different Loads

| Load at Bus 5 | sign(det$J_{LF}$) | sign(det$J_{AE}$) | Critical Eigenvalue(s) | Associated States |
|---|---|---|---|---|
| 4.3 | + | + | -0.1433±j2.0188 | $E'_{q1}$ & $R_{f1}$ |
| 4.4 | + | + | 0.0057±j2.2434 | $E'_{q1}$ & $R_{f1}$ |
| 4.5 | + | + | 0.3400±j2.5538 | $E'_{q1}$ & $R_{f1}$ |
| 4.6 | + | + | 1.1350±j2.8016 | $E'_{q1}$ & $R_{f1}$ |
| 4.7 | + | + | 2.5961±j2.2768 | $E'_{q1}$ & $R_{f1}$ |
| 4.8 | + | + | 9.2464, 1.8176 | $\delta_2$ & $\omega_2$, $E'_{q1}$ & $R_{f1}$ |
| 4.9 | + | - | 1.0542 | $E'_{q1}$ & $R_{f1}$ |
| 5.0 | + | - | 0.6298 | $E'_{q1}$ & $R_{f1}$ |
| 5.1 | + | - | 0.2463 | $E'_{q1}$ & $R_{f1}$ |
| 5.15 | + | - | -0.6832 | $E'_{q1}$ & $R_{f1}$ |
| 5.2 | Load flow does not converge | | | |

and is sensitive to the exciter mode. This eigenvalue returns to the left-half plane at the loading of approximately 5.15 pu at bus 5, and the system is again dynamically stable. For the load at bus 5 = 5.2 pu, the load flow does not converge. This phenomenon is pictorially indicated in the $P-V$ curve of Fig. 2 and the s-plane plot of Fig. 3.

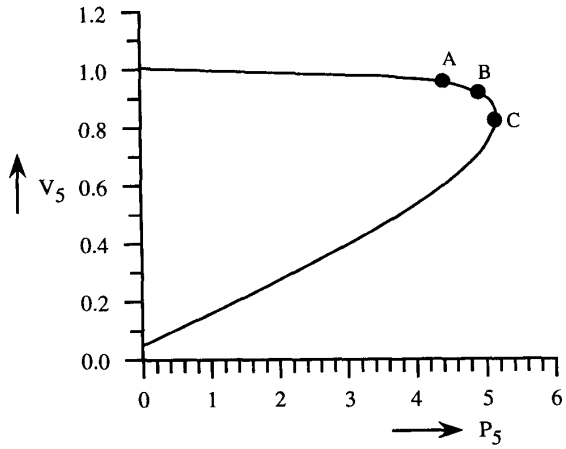


Figure 2: P-V curve for bus 5

At point A there is Hopf-bifurcation which has been shown to be subcritical. However a load flow solution still exists. In this region $E'_q$ & $R_f$ state variables are clearly dominant initially. As we approach towards B, $\delta_2$ & $\omega_2$ state variables start participating substantially in the trajectory of unstable eigenvalues as indicated in the Table 1.

Hopf bifurcation phenomena in power systems was first discussed in Ref. [15] for a single machine case. In their studies the electro-mechanical mode was the critical one. In studies relating to voltage collapse [16] it was shown that the exciter mode may go unstable first. We have shown that both exciter modes and electromechanical modes are critical in steady state stability and voltage collapse and that they both participate in the dynamic instability.

In conventional bifurcation theory terms, one can think of solving $g(x,y)=0$ for $y=h(x)$ and substituting this in the differential equation to get $\dot{x}=f(x,h(x))$. The change in sign of $detJ_{AE}$ is the instant when solution of $y$ is no longer possible. A concrete mathematical underpinning of this idea in the context of power systems is known as "Singularly induced bifurcation" in [17]. The concept of "Impasse surface" [18] may also be useful.

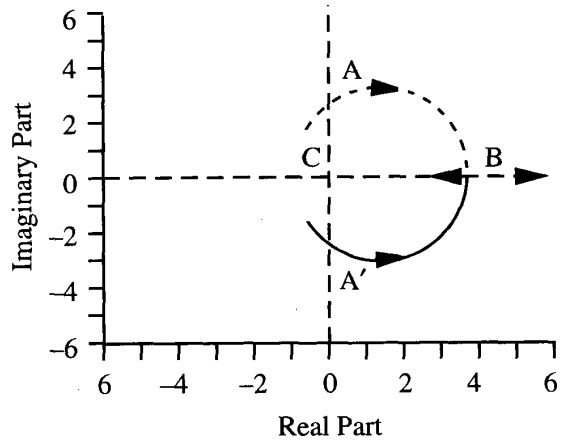


Figure 3: Critical modes of $\tilde{A}_{sys}$ as a function of the load at bus-5

Structural stability region is the same as the 'Typal' region discussed in [17]. The 'feasibility' region is the region around a point in the parameter space for which the system is small signal stable.

# 4 Effect of Static and Dynamic Load Modeling

In this section we discuss the effects of load modeling on structural stability. We emphasize the problem with the existence of solutions to the network/load model. We also present results concerning induction motor load models.

## 4.1 Bifurcations leading to loss of solution

The study of feasible operating points for use in steady-state stability studies has been addressed in the literature [19-23]. Beyond load flow, the topic of existence of solutions to network/load equations during dynamic analysis has been given somewhat less consideration in the literature. Interestingly, in [24] a distinction is made between bifurcations of the system algebraic equations and the bifurcations of the complete dynamic system. Whereas bifurcations of the dynamic system

may occur, bifurcations in the algebraic equations may indicate an unacceptable model at this point. A model must exhibit a real solution if it represents a physical system. One of the objectives in [18, 25] is to determine which static load models guarantee that a solution exists to the network/load equations. Specifically the common load model relating consumed power to an exponential of bus voltage magnitude is examined:

$$P(V) + jQ(V) = P_o V^{k_p} + jQ_o V^{k_q}. \quad (8)$$

Here we present a general result for multimachines systems.

Main Result: Assuming that the transmission network can be modeled by passive elements and loads are represented by (8) with parameters constrained by

$$P_o > 0$$
$$k_p\ ,\ k_q > 1$$

then the network/load quasi-static algebraic equations will exhibit at least one solution. The proof is given in [27].

Now we present a simple example in which the conditions above are made clear. Consider the single unity power factor load connected to a source through a lossless transmission line shown in Figure 4.

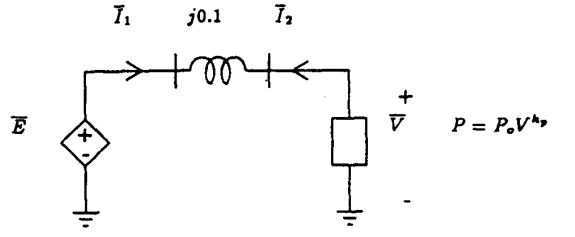


Figure 4: A single source/single load system

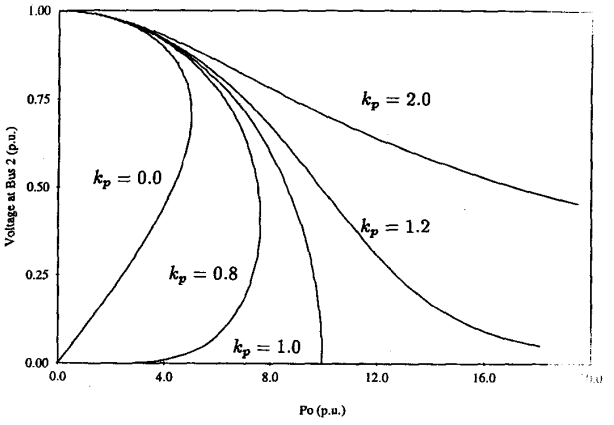


Figure 5: Load voltage vs. power coefficient

Assuming $E = 1$, the solutions for $V$ as a function of $k_p$ and $P_o$ are shown in Figure 5. We emphasize that a real solution for $V$ always exists for any $P_o > 0$ with $k_p > 1$ but may not exist for $k_p \leq 1$. This simple example helps to illustrate the bounds on the load model such that a solution exists.

To demonstrate explicitly how these results affect dynamic analysis, we perform a nonlinear simulation on the IEEE 10-machine/39-bus system. Initially the system is at its base loading, and the generators are modeled using a two-axis model with IEEE type I voltage regulator and a third-order turbine/governor model.

At the base loading level, the two most heavily loaded transmission lines are those connecting bus 21 to bus 36 and bus 39 to bus 36. The simulation involves disconnecting these lines. At time $t = 0$ sec the system is in steady state. At time $t = 1$ sec the line connecting buses 21 and 36 is removed. At time $t = 2$ sec the line connecting buses 39 and 36 is removed. The bus with the lowest voltage in the system is bus 21. In Fig. 6, the voltage at this bus is shown assuming different values for the load exponents. The trajectory labeled "$k = 0$" corresponds to the transients when all loads are modeled as constant power. The trajectory labeled "$k = 1$" corresponds to loads modeled as constant current magnitude at a constant power factor. The trajectory labeled "$k = 2$" corresponds to constant impedance loads. In the constant power case, the simulation fails to converge shortly after the second line is removed. The other two cases result in severe voltage conditions, yet the system is stable.

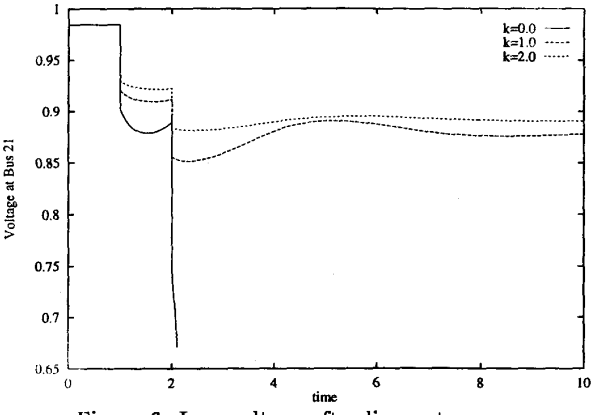


Figure 6: Low voltage after line outages

The simulations denoted by "$k = 1$" and "$k = 2$" correspond to possible power system transients. The simulation denoted by "$k = 0$ represents an impossible system transient since it fails to depict the transient after finite time. In actual commercial grade programs, this is avoided by switching the bus to constant impedance when the voltage falls below a certain value.

One may argue that the constant power load model (or any model $k_p, k_q \leq 1$) is valid for some (high) voltage levels but is not valid over the complete range of possible transient conditions. These types of models are typically used to represent induction motor presence in a power system. For voltage instability studies in which low voltages transients are expected, it is necessary to include more detailed models of induction motors to capture low voltage transient induction motor phenonena.

## 4.2 Bifurcations of the dynamic system

In this section we examine bifurcations in the total dynamic system using two different loads: a constant power model and an induction motor model.

The test systems are shown in Figs. 7 and 8. Both systems consist of a single generator connected to a single load through a lossless transmission line. In Fig. 7 the load is constant active power. In Fig. 8 the load is a compensated induction motor such that at a given operating point the resistor consumes 50% of the active power, the induction motor consumes

50% of the active power, and the shunt capacitance provides 100% compensation for reactive losses in the induction motor. The generator is represented by a two-axis model with an IEEE type I voltage regulator and a third-order turbine and governor model. The induction motor is represented by a third-order model in which the mechanical torque load is assumed to be linear to rotational speed. It is used as an aggregate to model many small induction motors in parallel.

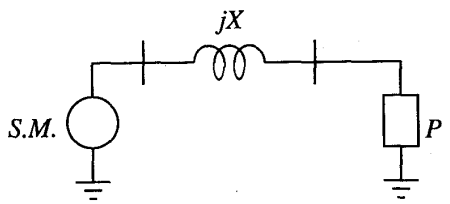


Figure 7: Single machine, constant active power load

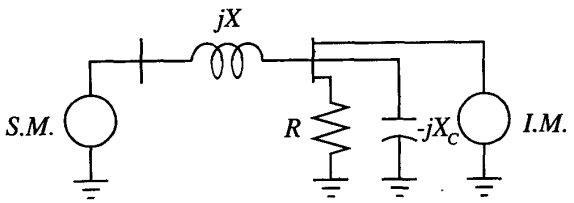


Figure 8: Compensated induction motor, unity power factor load

Detection of global bifurcations is difficult, so we begin by examining local bifurcations which can be detected from an eigenvalue analysis. In each case, the constant power load and the compensated induction motor load, the total active power of the load is increased until an eigenvalue crosses the imaginary axis of the complex plane. The eigenvalues at this point are given in Table 2, and the participation factors corresponding to the critical eigenvalues are shown in Table 3.

Table 2: Eigenvalues at Critical Levels of Load

| Constant P $P_L = 2.36pu$ | IM $P_L = 3.16pu$ |
|---|---|
| $0.0010 \pm j1.854$ | $0.0042 \pm j1.906$ |
| $-0.1852 \pm j0.2770$ | $-0.2067 \pm j0.2699$ |
| $-2.963$ | $-2.165$ |
| $-4.673$ | $-4.698$ |
| $-5.153 \pm j7.643$ | $-5.277 \pm j7.763$ |
| $-20.08$ | $-20.08$ |
| $-0.000$ | $0.000$ |
| N/A | $-10.96$ |
| N/A | $-47.41 \pm j48.57$ |

It is interesting to note the significance of Tables 2 and 3. Although the instability boundary occurs at different loadings for the constant power and the induction motor examples, qualitatively they are similar. The eigenvalues of the linearized systems have comparable values and the critical unstable eigenvalues are strongly related to the $E_q'$ and $R_f$ states in the generator model. The critical eigenvalues are a complex pair which cross the $j\omega$ axis at some point other than the origin. This is a "Hopf bifurcation." It corresponds to an intersection of an equilibrium point (a limit set) with a limit cycle (another limit set). It is expected that in the vicinity of this bifurcation either stable or unstable limit cycles should exist. It is called "subcritical" if the limit cycles are unstable and "supercritical" if the limit cycles are stable.

Table 3: Participation Factors for the Unstable Eigenvalues

| | P | IM |
|---|---|---|
| $\delta$ | 0.000 | 0.036 |
| $\omega$ | 0.000 | 0.038 |
| $E_q'$ | 0.439 | 0.287 |
| $E_d'$ | 0.124 | 0.094 |
| $E_{fd}$ | 0.101 | 0.061 |
| $R_f$ | 0.267 | 0.159 |
| $V_r$ | 0.070 | 0.043 |
| $T_m$ | 0.000 | 0.005 |
| $P_{ch}$ | 0.000 | 0.005 |
| $P_{sv}$ | 0.000 | 0.002 |
| $E_D'$ | | 0.126 |
| $E_Q'$ | | 0.083 |
| $s$ | | 0.060 |

The Hopf bifurcation for the constant power case has been studied and is subcritical [28]. This means that, as the loading is increased towards the bifurcation point, there is an unstable limit cycle which bounds the region of attraction of the stable system. Because there are ten state variables in the model, the entire phase plane cannot be visualized. Since the participation factors indicate that the critical mode is associated with the $E_q'$ and $R_f$ variables, view the $E_q' - R_f$ plane, keeping in mind that this is only a cross section of the entire state space. To examine the flow in this plane, a perturbation in the value of $E_q'$ is introduced and the resulting trajectories are plotted. Starting with a constant power load of $P_L = 2.35$ pu, the flow in Fig. 9 indicates an unstable limit cycle (solid line) around the locally stable equilibrium point. Trajectories lying inside the limit cycle spiral in towards the equilibrium; trajectories outside the limit cycle spiral outwards. Changing the loading to $P_L = 2.37$ pu, the flow in Fig. 10 does not show any limit cycle and the equilibrium point is unstable. All trajectories spiral outwards. This is consistent with the observation that this Hopf bifurcation is subcritical.

Now examine the induction motor example. A calculation of participation factors indicates that again the $E_q'$ and $R_f$ variables greatly affect the critical mode. At a loading of $P_L = 3.15$ pu, the flow is examined by introducing a perturbation in $E_q'$. The trajectory in Fig. 11 indicates that the equilibrium point is stable and is surrounded by two limit cycles, one unstable (inner) and one stable (outer). At a loading of $P_L = 3.17$ the trajectories in Fig. 12 indicate that there is one stable limit cycle around the unstable equilibrium point. The difference between these graphs is seen by the change in the behavior of the innermost trajectories. The innermost (and unstable) limit cycle shown in Fig. 11 does not appear in Fig. 12. The Hopf bifurcation is still subcritical; however, the presence of the stable limit cycle makes the dynamics significantly different from

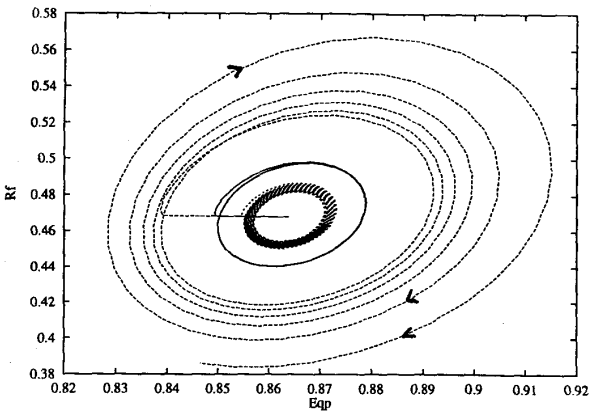


Figure 9: The constant power case, $P_L = 2.35pu$

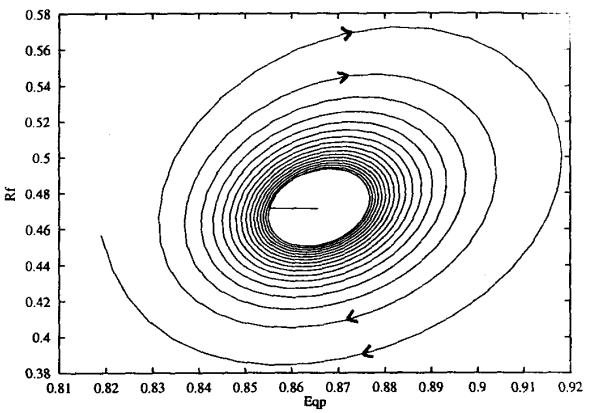


Figure 10: The constant power case, $P_L = 2.37pu$

those for the constant power case. Physically this means that the power system will exhibit sustained oscillations, either if the system is unstable or if a large disturbance is applied to the stable system.

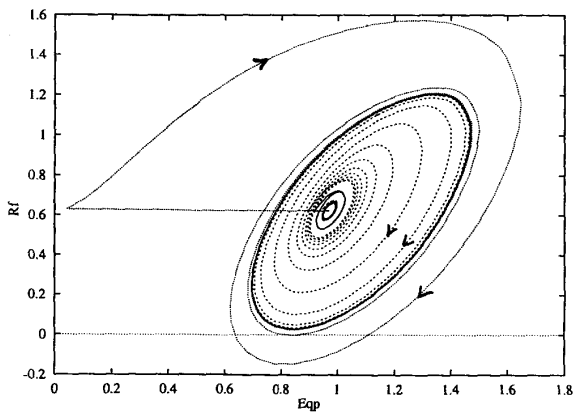


Figure 11: The IM model, $P_L = 3.15pu$

The differences between the flow in the phase planes are important. One of the traditional justifications for the constant power load model is the presence of induction motors.

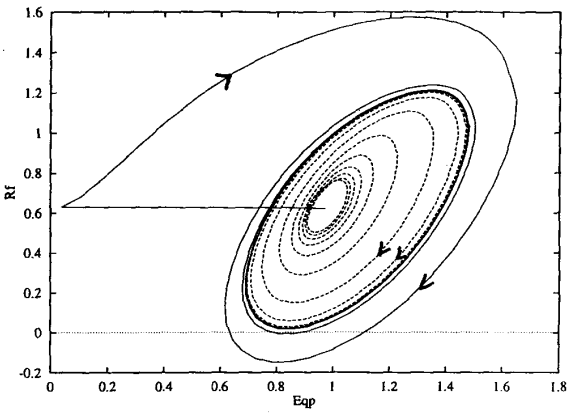


Figure 12: The IM model, $P_L = 3.17pu$

This may even be supported, in part, by the standard stability studies in which the eigenvalues of both models indicate an instability on the top half of the P-V curve. In addition, the participation factors indicate that this instability is associated with the $E_q^{'}$ and $R_f$ variables in the generator. However, the flow in state space shows that they are fundamentally different. As the constant power load is increased, the region of attraction around the equilibrium point shrinks, and after the bifurcation, the system is unstable with no limit cycles. When the eigenvalue becomes positive using induction motor parameters, the system exhibits stable limit cycles which appear as oscillations in the power system. The choice of load model greatly affects the dynamic behavior of the system.

Research into the effects of load modeling needs to be pursued further to gain a full understanding of the critical phenomena.

# 5 Conclusion

We summarize some of our results and indicate further areas of research.

1. Structural stability has been examined through several power system examples and related to bifurcation phenomena which have been reported in the literature. In particular, the concepts of global and local bifurcations were illustrated as structural instabilities. At this point, the task of finding regions in parameter space on the boundary of which the phase portraits change qualitatively is straightforward only for second order systems. Work is needed in this area to extend the application to realistic systems.
2. The maximum loadability for constant power load was compared to that of an induction motor. It was shown that while both models have a maximum load level, the dynamic nature of the induction motor limiting instability was considerably different than that of constant power. Both experienced Hopf bifurcations, but the induction motor instability was bounded by a stable limit cycle.

# 6 Acknowledgements

This work was performed as part of the EPRI Project RP 8010-21.

# References


[1] A. A. Andronov and L. Pontryagin, "Systems grossiers," Dukl. Akad. Nauk, SSSR, vol. 14, pp. 247-251, 1937.

[2] A. A. Andronov and C. E. Chaikin, *Theory of Oscillations*, Princeton University Press, Princeton, NJ, 1949.

[3] V. I. Arnold, *Geometric Methods In The Theory Of Ordinary Differential Equations*, Springer Verlag, New York, 1982.

[4] L. Perko, *Differential Equations and Dynamical Systems*, Springer Verlag, New York, 1991.

[5] J. Guckenheimer and P. Holmes, *Nonlinear Oscillations, Dynamical Systems and Bifurcation of Vector Fields*, Springer Verlag, New York, 1983.

[6] P. Varaiya, et al., *Bifurcation and Chaos In Power system: A Survey*, EPRI Report TR-100834, Aug. 1992.

[7] T. S. Parker and L. O. Chua, *Practical Numerical Algorithms For Chaotic Systems*, Springer Verlag, 1989.

[8] R. K. Bansal, *Estimation of Stability Domains for the Transient Stability Investigation of Power Systems*, Ph.D. Thesis, I.I.T., Kanpur, Aug. 1975.

[9] K. R. Padiyar, M. A. Pai and C. Radhakrishna, "A versatile system model for the dynamic stability analysis of power systems including HVDC links," *IEEE Transactions on Power Apparatus and Systems*, vol. 100, April 1981, pp. 1871-1880.

[10] P. Kundur, G. J. Rogers, D. Y. Wong, L. Wang and M. G. Lauby, "A comprehensive computer program package for small signal stability analysis of power systems," *IEEE Transactions on Power Systems*, vol. 5, no. 4, Nov. 1990, pp. 1076-1083.

[11] P. W. Sauer and M. A. Pai, "Power system steady-state stability and the load flow Jacobian," *IEEE Transactions on Power Systems*, vol. 5, no. 4, Nov. 1990, pp. 1374-1383.

[12] P. W. Sauer and M. A. Pai, "Modeling and simulation of multi-machine power system dynamics," *Control and Dynamic Systems: Advances in Theory and Application* (C. T. Leondes, Ed.), vol. 43, Academic Press, San Diego, CA, 1991.

[13] P. M. Anderson and A. A. Fouad, *Power System Control and Stability*, Iowa State University Press, Ames, IA, 1977.

[14] G. C. Verghese, I. J. Perez-Arriaga and F. C. Scheweppe, "Selective modal analysis with applications to electric power systems, Part I and II," *IEEE Transactions on Power Apparatus and Systems*, vol. PAS 101, no. 9, 1982, pp. 3117-3134.

[15] E. H. Abed and P. P. Varaiya, "Nonlinear oscillations in power systems," *International Journal of Electric Power and Energy Systems*, vol. 6, no. 1, pp. 37-43, 1984.

[16] C. Rajagopalan, B. Lesieutre, P. W. Sauer and M. A. Pai, "Dynamic aspects of voltage/power characteristics," *IEEE Transactions on Power Systems*, vol. 7, no. 3, pp. 990-1000, 1992.

[17] V. Venkatasubramaniam, H. Schattler and J. Zaborszky, "Voltage dynamics: study of a generator with voltage control, transmission and matched mw load," *IEEE Transactions on Automatic Control*, vol. 37, no. 11, Nov. 1992, pp. 1717-1733.

[18] I. A. Hiskens and D. J. Hill, "Failure modes of a collapsing power system," *Proc. of Bulk Power System Voltage Phenomena II – Voltage Stability and Security*, Deep Creek Lake, Maryland, Aug. 1991, pp. 53-63.

[19] J. Jarjis and F. D. Galiana, "Quantitative analysis of steady state stability in power networks," *IEEE Trans. on PAS*, vol PAS-100, No. 1, Jan. 1981, pp. 318-326.

[20] F.D. Galiana, "Power-voltage limitations imposed by the network structure of a power system," *Proc. of PICA*, 1975, pp. 356-363.

[21] F. F. Wu and S. Kumagai, "Steady-state security regions of power systems," *IEEE Trans. on Circuits and Systems*, vol. CAS-29, no. 11, Nov. 1982, pp. 703-711.

[22] P. Dersin and A.H. Levis, "Feasibility sets for steady-state loads in electric power networks," *IEEE Trans on PAS*, vol. PAS-101, no. 1, Jan. 1982, pp. 60-70.

[23] J-C. Chow, R. Fischl, and H. Yan, "On the evaluation of voltage collapse criteria," *IEEE Trans on power systems*, vol. 5, no. 2, May 1990, pp. 612-620.

[24] L. Fekih-Ahmed and H-D Chiang, "Analysis of voltage collapse in structure preserving models of power systems," *Proc of ISCAS*, San Diego, 1992, pp. 2525-2528.

[25] P.W. Sauer, B.C. Lesieutre, M.A. Pai, "Dynamic vs. Static aspects of voltage problems," *Proc. Bulk power system voltage phenomena II voltage stability and security*, Deep Creek Lake, MD, Aug. 1991, pp. 207-216.

[26] W. Xu and Y. Mansour, "Voltage stability analysis using genic dynamic load models," Paper 93 WM 185-9 PWRS, IEEE Winter Power Meeting, Colubus, OH, Jan. 31 - Feb. 5, 1993.

[27] B. C. Lesieutre, P. W. Sauer and M. A. Pai, "Sufficient conditions on static load models for network solvability," *Proceedings of the Twenty-Fourth Annual North American Power Symposium*, Reno, NV, Oct. 5-6, 1992, pp. 262-271.

[28] C. Rajagopalan, P. W. Sauer and M. A. Pai, "Analysis of voltage control systems exhibiting Hopf bifurcation," *Proceedings 28th IEEE Conference on Decisionand Control*, Tampa, FL, Dec. 13-15, 1989, pp. 332-335.


# Biographies

M. A. Pai (F'86) is a Professor of Electrical Engineering at the Universityof Illinois at Urbana-Champaign. His research interests are power systems stability and control.

Peter W. Sauer (S'73, M'77, SM'82, F'93) is a Professor of Electrical Engineering at the University of Illinois at Urbana-Champaign. He teaches courses and directs research in the electric power area.

Bernard C. Lesieutre (S'86, M'93) is an Assistant Professor of Electrical Engineering at MIT. His research interests include load modeling and power system analysis.

Rambabu Adapa (S'86, M'86, SM'90) is a project manager of the Power System Planning and Operation Program in Electric Power Research Institute. Dr. Adapa received his Ph.D. from the University of Waterloo, Canada.